INTERNATIONAL JOURNAL FOR NUMERICAL METHODS IN FLUIDS
Int. J. Numer. Meth. Fluids 2005; **49**:837–847
Published online 3 August 2005 in Wiley InterScience (www.interscience.wiley.com). DOI: 10.1002/fld.1026

Resonance behaviour of viscoelastic fluid in Poiseuille flow in the presence of a transversal magnetic field

Muhammad R. Mohyuddin[1,*,†] and T. Götz[2,‡]

[1]*Department of Mathematics, Quaid-i-Azam University 45320, Islamabad 44000, Pakistan*
[2]*Department of Mathematics, University of Kaiserslautern, P.O. Box 3049, D-67653, Kaiserslautern, Germany*

SUMMARY

The oscillatory flow of a viscoelastic fluid in a circular pipe under the influence of a transversal magnetic field is studied. Exact solutions for the axial velocity and flow rate are presented. The velocity enhancement and the resonance behaviour are analysed both numerically and asymptotically in the case of small pipe radii.

Approximations for the resonance frequencies and the achievable velocity enhancements are derived.

KEY WORDS: viscoelastic MHD flow; resonance; velocity enhancement

1. INTRODUCTION

Non-Newtonian fluids, among them viscoelastic fluids (e.g. oil, liquid polymers, rubber, colloidal suspension or blood) exhibit some remarkable phenomena due to their 'elastic' nature, see Reference [1] and references therein. Resonance phenomena of viscoelastic fluids appear in polymer processing, the so-called draw resonance, see References [2–7]. In References [8–10] pulsating viscoelastic flows and their resonance behaviour have been studied.

Since most fluids are electrically conducting or in technological applications exposed to magnetic fields, very often MHD effects cannot be neglected [10–14].

In the present work, we consider the unsteady flow of a viscoelastic fluid in a circular pipe [15]. It is assumed that a magnetic field perpendicular to the axis of the pipe is present, no external electric field is imposed and that the magnetic Reynolds number is small, such that induced magnetic fields can be neglected [11, 16]. Here we mention that in the presence

*Correspondence to: Muhammad R. Mohyuddin, Department of Mathematics, Quaid-i-Azam University 45320, Islamabad 44000, Pakistan.
†E-mail: m_raheel@yahoo.com
‡E-mail: goetz@mathematik.uni-kl.de

Contract/grant sponsor: ICTP/IAEA

Received 28 December 2004
Revised 18 April 2005
Accepted 24 April 2005

of electric and magnetic field one will have very general constitutive equations for the stress, free energy, etc. (see References [17, 18]) and this general constitutive equation for the stress is very complicated giving rise to highly nonlinear equations, which are not easy to solve. Actually, we are going to look at simplified MHD equations, which are similar to that in the case of classical MHD equations [19–21].

The purpose of our work is the mathematical and numerical study of these phenomena in order to obtain expressions for the axial velocity, velocity enhancement, flow rate and to analyse the resonance behaviour in the limit of small pipe radii.

The paper is organized as follows. In Section 2 we shortly recall the equations of magnetohydrodynamics and the constitutive relation of the upper convected Maxwell model. In Section 3 we solve the equation of motion for a viscoelastic MHD Poiseuille flow and introduce the velocity enhancement and flow rate. Section 4 deals with the resonance behaviour and its asymptotic analysis in case of small radii.

2. MHD EQUATIONS AND CONSTITUTIVE EQUATIONS OF VISCOELASTICITY

The unsteady flow of an incompressible fluid in the presence of a magnetic field is governed by equations of conservation of mass and momentum. These equations are

$$\nabla \cdot \mathbf{V} = 0 \tag{1}$$

$$\rho \frac{\mathrm{d}\mathbf{V}}{\mathrm{d}t} = \operatorname{div} \mathbf{T} + \mathbf{J} \times \mathbf{B} \tag{2}$$

in which $\mathbf{V}$ is the velocity vector, ρ is the density, $\mathrm{d}/\mathrm{d}t$ is the material time derivative, $\mathbf{T}$ is the stress tensor, $\mathbf{J}$ is the electric current density, and $\mathbf{B}$ is the total magnetic field $\mathbf{B} = \mathbf{B}_0 + \mathbf{b}$, where $\mathbf{b}$ is the induced magnetic field and $\mathbf{B}_0$ denotes the imposed magnetic field. In the absence of displacement currents, the Maxwell's equations [11, 16] and modified Ohm's law [22] can be written as

$$\begin{gathered} \nabla \cdot \mathbf{B} = 0, \quad \nabla \times \mathbf{B} = \mu_{\mathrm{m}} \mathbf{J}, \quad \nabla \times \mathbf{E} = -\frac{\partial \mathbf{B}}{\partial t} \\ \mathbf{J} = \sigma[\mathbf{E} + \mathbf{V} \times \mathbf{B}] \end{gathered} \tag{3}$$

where $\mathbf{E}$ is the electric field, μ_{m} is the magnetic permeability, and σ is the electric field conductivity.

The following assumptions are made in order to precede our discussion:

1. The density ρ, magnetic permeability μ_{m} and electric field conductivity σ, are considered constant throughout the flow field region.
2. Electric field conductivity σ is assumed finite.
3. Total magnetic field $\mathbf{B}$ is perpendicular to the velocity field $\mathbf{V}$ and the induced magnetic field $\mathbf{b}$ is negligible compared with the applied magnetic field $\mathbf{B}_0$ so that the magnetic Reynolds number is small [11, 16].
4. We assume a situation where no energy is added or extracted from the fluid by the electric field, which implies that there is no electric field present in the fluid flow region.

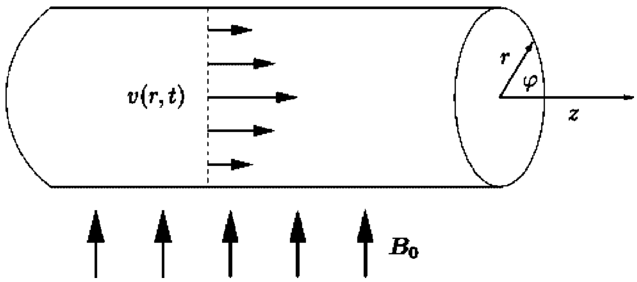

Figure 1. Sketch of the considered geometry.

Under these assumptions the electro-magnetic body force $\mathbf{J}\times\mathbf{B}$ becomes [11, 16]

$$\mathbf{J}\times\mathbf{B} = -\sigma B_0^2\mathbf{V} \tag{4}$$

For the stress tensor $\mathbf{T}$ of a viscoelastic fluid we use an upper convected Maxwell model with a discrete spectrum of relaxation times [1]. Considering a unidirectional Poiseuille flow in a cylindrical pipe, see Figure 1, and using cylindrical coordinates (r,φ,z), we obtain the following constitutive equation:

$$\begin{aligned}\tau(r,t) &= \sum_{k=1}^{K}\tau_k(r,t)\\ \left(1+\lambda_k\frac{\partial}{\partial t}\right)\tau_k(r,t) &= \eta_k\frac{\partial}{\partial r}v(r,t)\end{aligned} \tag{5}$$

where τ is the rz component of the extra stress tensor and v is the axial velocity. By K,λ_k and η_k, $k=1,2,\dots,K$ we denote the number of relaxation times in the spectrum, the kth relaxation time and partial viscosity, respectively. For $K=2$ and $\lambda_2=0$, one obtains the Oldroyd-B model and for $K=1$ and $\lambda_1=0$, the equations describe a Newtonian fluid.

3. VISCOELASTIC MHD POISEUILLE FLOW

Consider a unidirectional Poiseuille flow in the presence of a transversal magnetic field, see Figure 1. In cylindrical coordinates, the equation of motion reads as

$$\rho\frac{\partial}{\partial t}v(r,t) = -\frac{\partial p(t)}{\partial z} + \frac{1}{r}\frac{\partial(r\tau)}{\partial r} - \sigma B_0^2 v \tag{6}$$

where p is the scalar pressure. The boundary conditions for the velocity are

$$\begin{aligned}&v(r=R,t)=0\\ &v \text{ is finite when } r\to 0\end{aligned} \tag{7}$$

where R is the radius of the pipe.

Let the pressure gradient oscillate with frequency ω and amplitude p_1, i.e.

$$\frac{\partial p(t)}{\partial z} = p_1 e^{i\omega t} \tag{8}$$

A stationary oscillating solution of Equations (5) and (6) is sought in the form

$$v(r,t) = u_\omega(r)e^{i\omega t} \tag{9}$$

Using Equations (8) and (9) into Equations (5) and (6) we obtain the equation satisfied by u_ω as follows

$$r^2 u''_\omega + r u'_\omega + (\xi r)^2 u_\omega = \frac{-p_1(\xi r)^2}{\rho(n + i\omega)} \tag{10}$$

where prime denotes the differentiation with respect to r and $n = \sigma B_0^2/\rho$.

The solution of Equation (10) satisfying conditions (7) gives the axial velocity as follows:

$$u_\omega(r) = -\frac{p_1}{\rho(n + i\omega)}\left[1 - \frac{J_0(r\xi)}{J_0(R\xi)}\right] \tag{11}$$

where

$$\xi = \left[-(n + i\omega)\left(\sum_{k=1}^{K} \frac{\mu_k}{1 + i\omega\lambda_k}\right)^{-1}\right]^{1/2}, \quad \mu_k = \frac{\eta_k}{\rho}$$

and J_k is the kth order Bessel function [23].

In the case of constant pressure gradient, i.e. $\omega = 0$, we obtain

$$u_0(r) = -\frac{p_1}{\eta\alpha^2}\left[1 - \frac{I_0(r\alpha)}{I_0(R\alpha)}\right] \tag{12}$$

where

$$\eta = \sum_{k=1}^{K} \eta_k, \quad \alpha^2 = \frac{\sigma B_0^2}{\eta} = \frac{n\rho}{\eta}$$

and I_k is the kth order modified Bessel function [23]. The parameter α is also known as the Hartmann number [16].

3.1. Flow rate

The flow rate and the average flow rate are defined by

$$Q(t) = 2\pi \int_0^R v(r,t) r \, dr \tag{13}$$

$$\tilde{Q} = \lim_{T\to\infty} \frac{1}{T} \int_0^T Q(t) \, dt \tag{14}$$

For a constant pressure p_0, Equations (11) and (12) in (14) lead to the flow rate

$$\tilde{Q}_\alpha = \frac{2\pi R p_0}{\eta\alpha^3}\left(\frac{I_1(R\alpha)}{I_0(R\alpha)} - \frac{\alpha R}{2}\right) \tag{15}$$

Note that an oscillating pressure gradient leads to a zero mean flow rate.

Comparing the average flow rate $\tilde{Q}_\alpha$ to the flow rate $\tilde{Q}_0$ in the absence of a magnetic field, we obtain the ratio

$$B = \frac{\tilde{Q}_\alpha}{\tilde{Q}_0} = \frac{16}{R^3\alpha^3}\left(\frac{\alpha R}{2} - \frac{I_1(R\alpha)}{I_0(R\alpha)}\right) = 1 - \frac{R^2\alpha^2}{6} + O(R^4\alpha^4) \tag{16}$$

Clearly, the presence of a magnetic field diminishes the flow rate, see Figure 2.

3.2. Velocity enhancement

We introduce the coefficient A of the velocity enhancement as the ratio of the amplitude of the velocity oscillations on the tube axis and the velocity when the pressure gradient is constant and equal to p_1, that is

$$A(\omega) = \left|\frac{\text{amplitude of velocity oscillation on the axis}}{\text{velocity on the axis for constant pressure gradient}}\right| = \left|\frac{u_\omega(0)}{u_0(0)}\right| \tag{17}$$

Inserting Equations (11) and (12) we obtain

$$A(\omega) = \frac{\eta\alpha^2}{\rho|n + \mathrm{i}\omega|}\frac{|1 - J_0(R\xi)^{-1}|}{|1 - I_0(R\alpha)^{-1}|}$$

Let us consider the case of a single relaxation time, i.e. $K = 1$. It is useful to introduce the dimensionless parameters

$$\tilde{R} = \frac{R}{\sqrt{\mu\lambda}}, \quad \tilde{\omega} = \omega\lambda, \quad \mu = \frac{\eta}{\rho}, \quad \tilde{\alpha} = \alpha\sqrt{\mu\lambda}$$

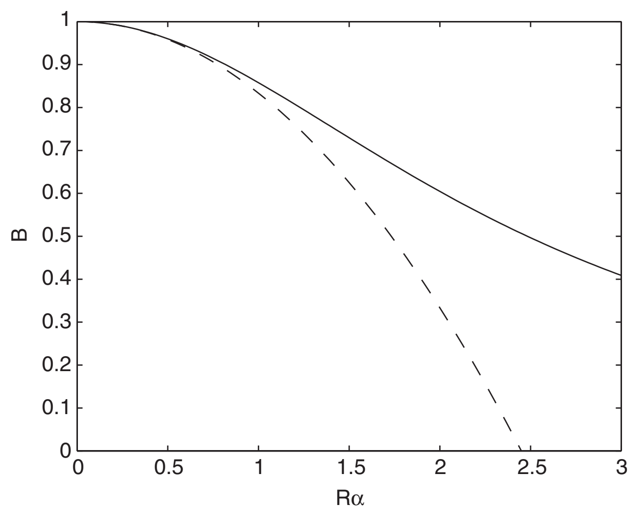

Figure 2. Decrease of the flow rate in the presence of a magnetic field. Shown are the ratio B ('—') according to (16) and its asymptotic approximation ('- - - -') vs $R\alpha$.

We see that $A(\omega)$ depends solely on the parameters $\tilde{R}$ and $\tilde{\alpha}$. Skipping the tildes we obtain

$$A_{R,\alpha}(\omega) = \frac{1}{\sqrt{1+\omega^2/\alpha^4}} \frac{|1 - J_0(R\xi)^{-1}|}{|1 - I_0(R\alpha)^{-1}|} \tag{18}$$

where

$$\xi = \sqrt{\omega^2 - \alpha^2 - \mathrm{i}\omega(1+\alpha^2)}$$

In the case of a vanishing magnetic field ($\alpha = 0$), the velocity enhancement is determined by

$$A_{R,0}(\omega) = \frac{|1 - J_0(R\sqrt{\omega^2 - \mathrm{i}\omega})^{-1}|}{\omega} \lim_{\alpha \to 0} \frac{\alpha^2 |I_0(R\alpha)|}{|I_0(R\alpha) - 1|} = \frac{4|1 - J_0(R\sqrt{\omega^2 - \mathrm{i}\omega})^{-1}|}{R^2 \omega} \tag{19}$$

To discuss the influence of the viscoelasticity on the velocity enhancement, the above scaling is not adequate, since it does not permit to consider the case $\lambda = 0$, i.e. pure viscous behaviour. Therefore we propose a different set of dimensionless parameters

$$\tilde{R} = R\sqrt{\frac{n}{\mu}}, \quad \tilde{\omega} = \frac{\omega}{n}, \quad \beta = n\lambda \tag{20}$$

Using these parameters and skipping the tilde, the velocity enhancement reads as

$$A_{R,\beta}(\omega) = \frac{1}{\sqrt{1+\omega^2}} \frac{|1 - J_0(R\sqrt{\beta\omega^2 - 1 - \mathrm{i}\omega(1+\beta)})^{-1}|}{|1 - I_0(R)^{-1}|} \tag{21}$$

This form now easily allows one to consider the viscous case $\lambda = 0$, i.e. $\beta = 0$. Figure 3 shows the graph of $A_{R,\beta}(\omega)$ for $R = 0.25$ and $\beta \in \{0.2,\ 0.15,\ 0.10\}$. Note that for $\beta \to 0$ (pure viscous behaviour), the resonance structure of the velocity enhancement disappears.

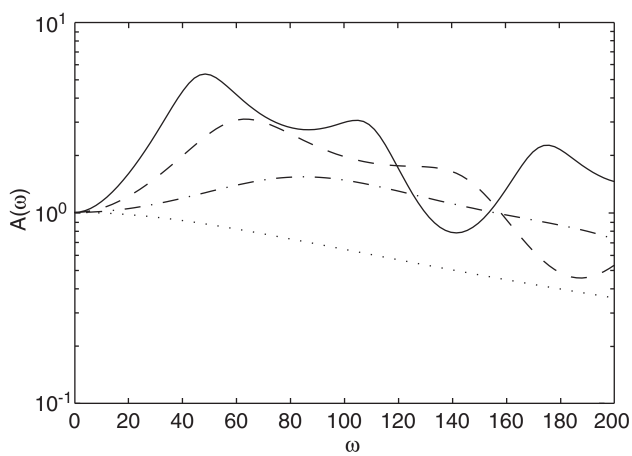

Figure 3. Velocity enhancement $A(\omega)$ vs frequency ω. Shown are the graphs for $R = 0.25$ and $\beta = 0.2$ ('—'), $\beta = 0.15$ ('– –'), $\beta = 0.1$ ('–·') and $\beta = 0$ ('…').

4. RESONANCE BEHAVIOUR

The velocity enhancement is given by Equation (18). In Reference [9] the resonance behaviour of A in the absence of a magnetic field $\alpha = 0$ has been studied. In this section we analyse the resonance if a magnetic field is present. Figure 4 shows the graph of $A_{R,\alpha}$ for $R = 0.3$ and $\alpha \in \{0, 1, 1.5, 2.5\}$. The different maxima of A are clearly visible. We also observe that for α increasing, every second maximum disappears. For a given value of R we will consider the question, for which value of α the second maximum disappears.

In case of small pipe diameters $R \ll 1$ we are interested in an asymptotic analysis of the position and the height of the maxima $\hat{\omega}$ and the minima $\breve{\omega}$ in dependence of the MHD-parameter α. We assume that $R \ll 1$ and $\alpha = O(1)$ and introduce the new frequency $x = R\omega$. Finding x such that A is maximal is equivalent to maximizing

$$h(x) = \frac{1}{x^2 + R^2\alpha^4}\left(1 - \frac{1}{J_0(R\xi)}\right) \times \text{conjugate}\left(1 - \frac{1}{J_0(R\xi)}\right) \tag{22}$$

Plugging the ansatz $x = x_0 + Rx_1 + \cdots$ into the condition $\mathrm{d}h/\mathrm{d}x = 0$ we obtain in zeroth order equation

$$-2\alpha^2 x(J_0(x) - 1)J_0(x)(J_0(x)^2 - J_0(x) + xJ_1(x)) = 0$$

with the solutions

$$x = 0, \quad x = j_k \quad \text{and} \quad x = \varsigma_k$$

where j_k is the kth positive zero of J_0, $j_1 = 2.4048$, $j_2 = 5.5201$ and ς_k is the kth zero of $J_0(x)^2 - J_0(x) + xJ_1(x)$, $\varsigma_1 = 4.1648$, $\varsigma_2 = 7.1145$. The solutions j_k correspond to the maxima of A whereas the minima are located at ς_k.

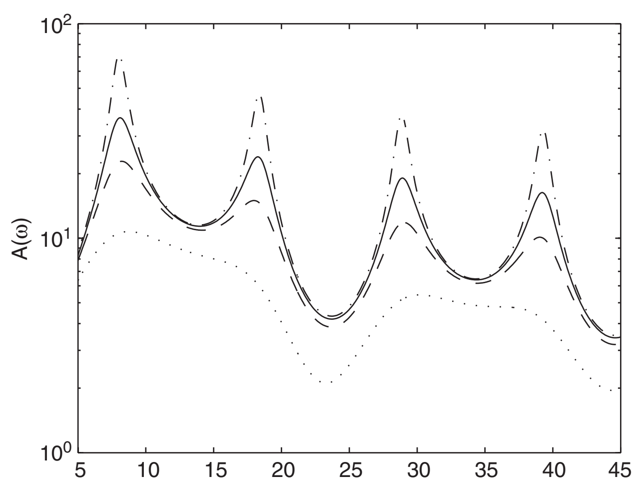

Figure 4. Velocity enhancement $A(\omega)$ vs frequency ω. Shown are the graphs for $R = 0.3$ and $\alpha = 0$ ('–·'), $\alpha = 1$ ('—'), $\alpha = 1.5$ ('– –') and $\alpha = 2.5$ ('…').

Computing the higher order terms we obtain

$$\hat{x}_k = j_k + \frac{J_1(j_k) j_k (\alpha^2+1)^2 - (\alpha^4+1)}{4 j_k} R^2 + \cdots \tag{23}$$

$$\hat{\omega}_k = \frac{j_k}{R} + \frac{J_1(j_k) j_k (\alpha^2+1)^2 - (\alpha^4+1)}{4 j_k} R + \cdots \tag{24}$$

$$\hat{\omega}_1 = \frac{2.405}{R} + (0.02579(\alpha^4+1) + 0.2579\alpha^2) R + \cdots \tag{25}$$

$$A_{R,\alpha}(\hat{\omega}_k) = \frac{8}{|J_1(j_k)| j_k (\alpha^2+1)} + O(1) \tag{26}$$

$$A_{R,\alpha}(\hat{\omega}_1) = \frac{6.406}{\alpha^2+1} R^{-2} + \frac{0.6026(\alpha^4+1) + 0.6516\alpha^2}{\alpha^2+1} + \cdots \tag{27}$$

for the maxima and

$$\check{x}_1 = \varsigma_1 + (0.03783\alpha^4 + 0.2125\alpha^2 + 0.05459) R^2 + \cdots \tag{28}$$

$$A_{R,\alpha}(\check{\omega}_1) = \frac{3.48}{R} - (0.2774\alpha^4 + 0.5407\alpha^2 + 0.2633) R + \cdots \tag{29}$$

for the first minimum.

In the case $\alpha = 0$ (no magnetic field), the above results reduce to the formulas given in Reference [9].

Figures 5 and 6 show the relative errors of the asymptotic expansion for the frequency $\hat{\omega}_1$ and, respectively, the height $A_{R,\alpha}(\hat{\omega}_1)$ of the first maximum for different values of α. The irregular behaviour of the graphs of $\hat{\omega}_1$ for small values of R are caused by the numerical maximization routine since the maximum is localized up to a tolerance of 10^{-6}.

To discuss the question for which value α_0 of the MHD-parameter the second maximum $\hat{\omega}_2$ disappears, we consider the case $R = 0.3$. Figure 7 shows the frequencies of the first and second maximum and the minimum separating them for values α ranging between 0.5 and 3. For $\alpha = \alpha_0 \sim 2.22$ the minimum $\check{\omega}_1$ and the second maximum $\hat{\omega}_2$ approach each other and disappear for larger values of α.

To compute an approximate value for α_0, we have different alternatives. First, setting the asymptotic expansion (23) for the frequency of the second maximum equal to expansion (28) for the frequency of the minimum yields

$$\alpha_{0,\omega} = \frac{1.684}{\sqrt{R}} - 0.337\sqrt{R} + \cdots \tag{30}$$

Second, we can set the expansion for the height of the maximum equal to the expansion for the height of the minimum and obtain the alternative approximation

$$\alpha_{0,A} = \frac{1.106}{\sqrt{R}} - 0.452\sqrt{R} + \cdots \tag{31}$$

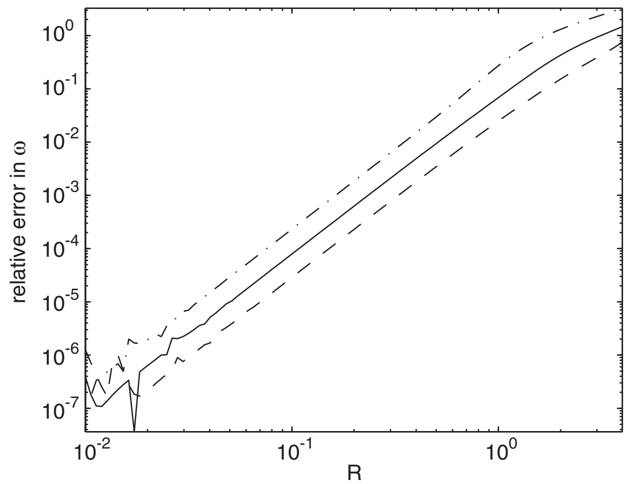

Figure 5. Relative error of the asymptotic expansion for the frequency of the first maximum. The different graphs corresponding to $\alpha = 0.5$ ('_ _'), $\alpha = 1$ ('_'), $\alpha = 1.5$ ('–·').

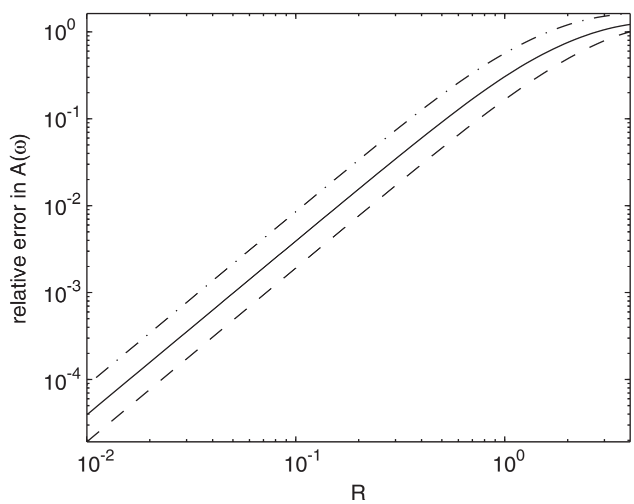

Figure 6. Relative error of the asymptotic expansion for the height of the first maximum. The different graphs corresponding to $\alpha = 0.5$ ('_ _'), $\alpha = 1$ ('_'), $\alpha = 1.5$ ('–·').

A direct computation of α_0 based on (22) seems to be intractable due to the high algebraic complexity. Figure 8 provides a comparison of Equations (30) and (31) with numerical simulations. All three graphs show clearly the $O(R^{-1/2})$-behaviour of α_0.

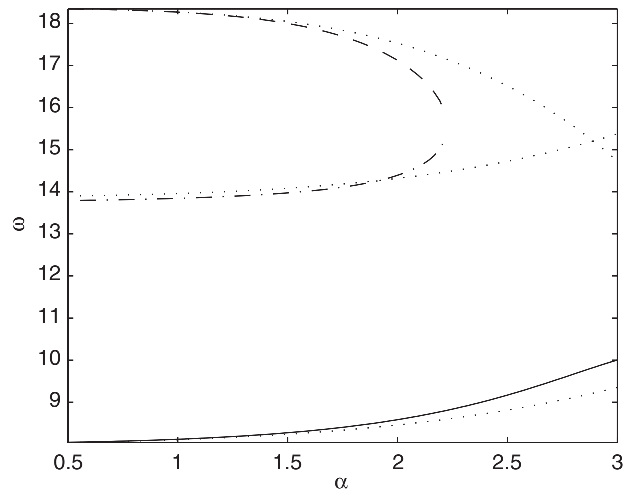

Figure 7. Frequencies of the first maximum $\hat{\omega}_1$ ('—'), the second maximum $\hat{\omega}_2$ ('– –'), and the minimum $\check{\omega}_1$ ('–·') separating them vs α. The dotted lines represent the asymptotic expansions for the respective quantities.

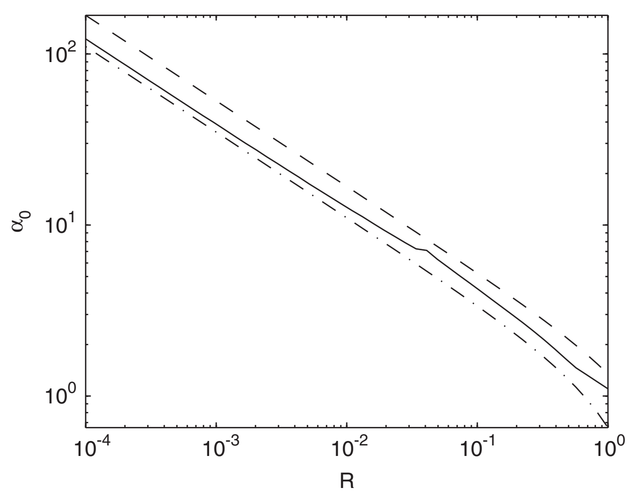

Figure 8. Critical MHD-parameter α_0 vs R. Shown are results from numerical simulations ('—') and the approximations (30) ('– –') and (31) ('–·').

5. CONCLUSIONS

We have considered the oscillatory flow of a viscoelastic fluid in a circular pipe under the influence of a transversal magnetic field. Comparing the exact solutions for the axial velocity to the velocity of a nonoscillatory flow shows a very pronounced resonance behaviour. In the case of small pipe radii, the resonance frequencies and the achievable velocity enhancements have been studied using asymptotic analysis. A remarkable phenomenon is that for increasing MHD-parameter, the resonance behaviour changes and certain maxima disappear. The limiting frequency, for which this occurs has been both approximately estimated and numerically computed. A precise prediction of the critical value for the MHD-parameter is still lacking and will be subject of further research.

ACKNOWLEDGEMENTS

The first author greatly acknowledges the ICTP/IAEA grant under the STEP programme for supporting his stay at ICTP, Trieste, Italy due to which this work became possible. He is thankful to Prof. K. R. Rajagopal for his valuable comments in order to improve the worth of the paper. We would also like to thank the director of ICTP, Prof. K. R. Sreenivasan for his support and cooperation.

REFERENCES

1. Bird RB, Armstrong RC, Hassager O. *Dynamics of Polymeric Liquids*, vol. 1. Wiley: New York, 1977.
2. Fisher RJ, Denn MM. A theory of isothermal melt spinning and draw resonance. *AIChE Journal* 1976; **22**(2): 236–246.
3. Petrie CJS, Denn MM. Instabilities in polymer processing. *AIChE Journal* 1976; **22**(2):209–236.
4. Anturkar NR, Co A. Draw resonance in film casting of viscoelastic fluids: a linear stability analysis. *Journal of Non-Newtonian Fluid Mechanics* 1988; **28**(3):287–307.
5. Cao J. Numerical simulation of draw resonance in melt spinning of polymer fluids. *Journal of Applied Polymer Science* 1993; **49**:1759–1768.
6. van der Hout R. Draw resonance in isothermal fibre spinning of Newtonian and power-law fluids. *European Journal of Applied Mathematics* 2000; **11**:129–136.
7. Lee JS, Jung HW, Kim SH, Hyun JC. Effect of fluid viscoelasticity on the draw resonance dynamics of melt spinning. *Journal of Non-Newtonian Fluid Mechanics* 2001; **99**(2–3):159–166.
8. Siginer A. On the pulsating pressure gradient driven flow of viscoelastic liquids. *Journal of Rheology* 1991; **35**(2):271–311.
9. Andrienko YA, Siginer DA, Yanovsky YG. Resonance behavior of viscoelastic fluids in Poiseuille flow and application to flow enhancement. *International Journal of Non-Linear Mechanics* 2000; **35**:95–102.
10. El-Shenawey EF, Elbarbary EME, Afifi NAS, Elshahed M. MHD flow of an elastico-viscous fluid under periodic body acceleration. *International Journal of Mathematics and Mathematical Sciences* 2000; **23**(11):795–799.
11. Shercliff JA. *A Textbook of Magnetohydrodynamics*. Pergamon Press: Oxford, 1965.
12. Ray RN, Samad A, Chaudhury TK. Low Reynolds number stability of MHD plane Poiseulle flow of an Oldroyd fluid. *International Journal of Mathematics and Mathematical Sciences* 2000; **23**(9):617–625.
13. Usha R, Gotz T. Spinning of a liquid film from a rotating disc in the presence of a magnetic field—a numerical solution. *Acta Mechanica* 2001; **147**(1–4):137–151.
14. Sarpakaya T. Flow of non-Newtonian fluids in a magnetic field. *AIChE Journal* 1961; **7**(2):324–328.
15. Siginer DA, Valenzuela-Rendon A. Energy considerations in the flow enhancement of viscoelastic liquids. *ASME Journal of Applied Mechanics* 1993; **60**:344–352.
16. Davidson PA. *An Introduction to Magnetohydrodynamics*. Cambridge University Press: Cambridge, MA, 2001.
17. Eringen AC, Maugin GA. Electrodynamics of Continua I. *Foundations and Solid Media*, 1990.
18. Siginer DA. Oscillating flow of a simple fluid in a pipe. *International Journal of Engineering Science* 1991; **29**:1557–1567.
19. Rajagopal KR, Ruzicka M. On the modeling of electrorheological materials. *Mechanics Research Communications* 1996; **23**:401–407.
20. Ruzicka M. Flow of shear dependent electrorheological fluids: fluids. *CRAS* 1999; **329**:393–398.
21. Rajagopal KR, Ruzicka M. Mathematical modelling of electrorheological materials. *Continnum Mechanics and Thermodynamics* 2001; **13**:59–78.
22. Sherman A, Sutton GW. *Engineering Magnetohydrodynamis*. McGraw-Hill: New York, 1965.
23. Abramowitz M, Stegun IA. *Handbook of Mathematical Functions*. Dover: New York, 1972.

